Degradation study of InGaAsN PIN solar cell under 1 MeV electron irradiation

Maxime Levillayer, Sophie Duzellier, Thierry Nuns, Christophe Inguimbert, Tifenn Lecocq, Inès Massiot, Alexandre Arnoult, Corinne Aircadi, S. Parola, Guilhem Almuneau, et al.

Degradation study of InGaAsN PIN solar cell under 1 MeV electron irradiation

M. Levillayer[1,2,3], S. Duzellier[1], T. Nuns[1], C. Inguimbert[1], T. Le Cocq[1], R. Rey[1], C. Pons[1], F. Olivié[2], I. Massiot[2], A. Arnoult[2], C. Aicardi[3], S. Parola[4], G. Almuneau[2], L. Artola[1]

Abstract— **Degradation of InGaAsN *pin* subcell under 1 MeV electron irradiation was studied by characterizing solar cells and dilute nitride bulk layers before and after irradiation. The measurements show that these cells retain more than 94% of their original photocurrent after an 10^{15} cm^{-2} electron-irradiation. Moreover, no significant degradation of the optoelectronic properties is observed after irradiation.**

Index Terms— **Degradation, dilute nitrides, electrons, InGaAsN, irradiation, MJSC, solar cell, DLTS, PL, EQE**

I. INTRODUCTION

Multi-junction solar cells (MJSC) based on III-V materials offer today the highest conversion efficiency of all solar technologies, as their structure leads to the optimal usage of the solar spectrum. MJSC are then of prime interest for space applications where delivered power over charge ratiois the key parameter. Today's space solar cell market is dominated by the GaInP/(In)GaAs/Ge tri-junction cell lattice-matched to its substrate, with 28-30 % efficiency [1]. Both the architecture and the materials of this standard tri-junction cell have already been optimized and room for improvement is now extremely limited.

Changing or adding subcells appears then to be necessary in order to overpass the 30 % efficiency level. Theoretical calculations with the optimal bandgap combination point out the need to develop a 1 eV subcell to improve the spectral overlapping [2]. One way to improve the structure is to subtstitute the Ge for a 1 eV material in the bottom cell. Another possibility is to fabricate a 4-junction solar cell by introducing a 1 eV subcell between the GaAs and the Ge ones.

A major requirement for the 1 eV subcell is that the material needs to be lattice-matched on GaAs or Ge, insuring the best crystalline quality. Dilute nitride ($In_xGa_{1-x}As_{1-y}N_y$) alloys have been proposed as candidates for this application as both their bandgap and their lattice parameter can be tuned by varying the indium and nitrogen contents [3]-[5]. As a notable proof-of-concept, Solar Junction reported in 2011 a world record efficiency (at the time) of 43.5 % under concentration for a tri-junction incorporating an InGaAsN-based bottom cell [6].

Furthermore, space applications require the subcell to be radiation hard since constant irradiation inevitably leads to cell degradation. This degradation can be particularly problematic for MJSC since its subcells are connected in series and thus each cell is required to generate the same amount of photocurrent.

Several degradation studies have already been reported for InGaAsN cells but the irradiations were carried out on non-optimized cells (regarding both the material and the architecture) grown by metal organic vapor phase epitaxy (MOVPE) [7]-[9]. More recent studies reported on quasi-optimized structures achieving short-circuit current density (J_{sc}) higher than 15 mA/cm² under integrated illumination conditions (AM0 > 870 nm [10] and AM1.5 > 830 nm [11]). These cells are based on a *n-i-p* design which strongly relies on a field-aided collection regime. Moreover, the dilute nitride material quality was improved by using molecular beam epitaxy (MBE) instead of MOVPE, leading to lower background carrier concentration.

As lattice-matching and current-matching conditions can be fulfilled, InGaAsN subcell integration into MJSC is feasible [6], [12]. It is now crucial to quantify and understand the degradation of InGaAsN under standard irradiation conditions. To do so, we propose to study the InGaAsN subcell degradation by combining the current-voltage characterization (I-V), the external quantum efficiency (EQE), the deep level transient spectroscopy (DLTS) and the photoluminescence (PL) at the beginning of life (BOL) and after samples irradiation with a 1 MeV electrons beam.

II. EXPERIMENTAL METHOD

A. InGaAsN cell and diode fabrication for DLTS characterization

The InGaAsN *p-i-n* cell structure is grown by MBE on a 4-inch n-GaAs (001) substrates. The device structure is composed of a *p-i-n* GaAs/InGaAsN/GaAs junction and include a n-$Al_{0.4}Ga_{0.6}$As back surface field (BSF), a p-$Al_{0.4}Ga_{0.6}$As window layer capped with a p$^+$ GaAs layer (Fig. 1a). TABLE I. summarizes the InGaAsN growth conditions of this series of studied cells, labelled as A, B, C and D. Other growth parameters were kept constant. The composition of the InGaAsN active layer was set to 4.5 % for In and ≈ 1.6 % for N corresponding to the lattice-matched condition. No rapid thermal processing (RTP) was performed on these wafers.

Furthermore, a 1.5 µm-thick non-intentionally doped (NID) InGaAsN bulklayers are grown on 4-inch n-GaAs (001) substrate with different As/III ratios for PL and DLTS characterizations. The growth conditions of these samples (E and F) can be found in TABLE I. Some of these samples were annealed at 750 °C for 30 s before being processed while others were processed as-grown. Electrochemical voltage capacitance measurements show that the InGaAsN layers are n-doped with concentrations ranging from 3.10^{16} to 1.10^{17} cm^{-3}.

TABLE I.   INGAASN GROWTH CONDITIONS

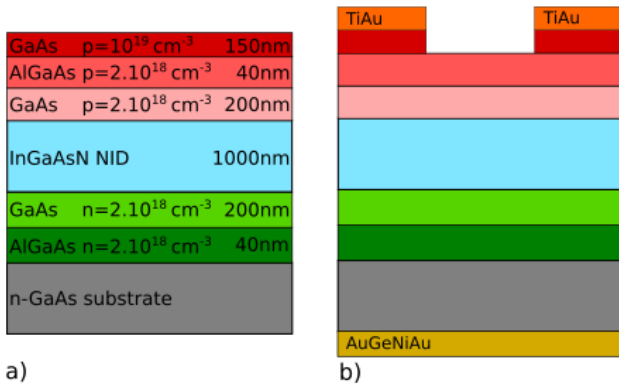| Wafer	Structure	Surfactant	Growth Temperature	As/III
A		Bi	465°C	12
B	p-i-n cells	Ø	465°C	12
C		Ø	445°C	10
D		Ø	485°C	10
E	InGaAsN monolayer	Ø	465°C	11
F		Ø	465°C	8

Fig. 1 Structure of the epitaxial stack of the InGaAsN cell (a) and cut view after processing steps (b)

AuGeNi/Au metallization was carried out on the backside surface of the substrate by sputtering deposition and a Ti/Au metallic grid was deposited on the surface front by e-beam evaporation followed by a lift-off step. Wafers were then annealed at 350 °C during 90 s in order to achieve good ohmic contacts. Wet etching was performed using H_3PO_4/H_2O_2 to form mesa structures to isolate each cell. The GaAs cap layer was afterwards selectively removed using $C_6H_8O_7/H_2O_2$. No anti-reflective coating (ARC) was deposited. Wafers were finally cleaved in 0.25 cm² and 1 cm² cells respectively for EQE and *I-V* measurements, with grid densities ranging from 0 to 10 %. The processed cell structure cut view is shown in Fig. 1b.

The InGaAsN bulk layers were processed with the same technological steps as the solar cells in order to fabricate Schottky diodes (NID InGaAsN / TiAu) for DLTS measurements.

B. Irradiation conditions

Cells and samples A to F were irradiated in the MIRAGE facility at ONERA with a Van de Graaff accelerator providing 1 MeV electron beam [13]. The electron flux was maintained below 5.10^{10} e$^-$/cm²/s ($\approx$ 8 nA/cm²) in order to to avoid irradiation-induced overheating as samples were not thermally regulated during irradiation. However, they were mounted on aluminum nitride support and copper plate (see Fig. 2), which both have high thermal conductivity. The irradiation chamber was at room temperature and the pressure was set tbelow 10^{-6} mbar.

Four solar cells thereafterlabelled A1, B1, D1 and G1 were irradiated four times, with cumulative fluences of respectively 5.10^{13}, 1.10^{14}, 5.10^{14} and 1.10^{15} e$^-$/cm², allowing us to measure their *I-V* characteristics at various fluence levels. The rest of the samples was irradiated in one step up to 1.10^{15} e$^-$/cm². GaAs *p-n* cells were irradiated as degradation references (G cells).
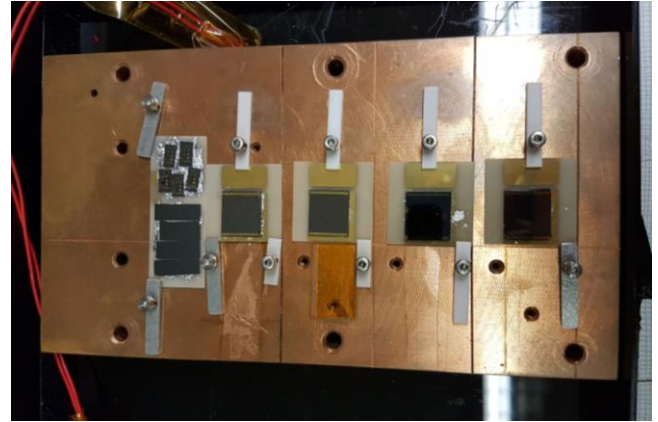

Fig. 2 Cells and samples for PL mounted on their holders for irradiation

III. RESULTS AND DISCUSSION

A. InGaAsN solar cells response to irradiation

The *I-V* characteristics were measured with an Oriel solar simulator equipped with a Xenon lamp and a AM0 filter, preliminary calibrated with a reference tri-junction cell from Azur Space. Fig. 3a shows the *J-V* characteristics of the GaAs reference before and after the different steps of irradiation. As commonly reported, J_{sc} decreases because of defect introduction which shortens the minority carrier diffusion length leading to a reduction of the collection efficiency [14], [15]. The normalized J_{sc} values are plotted as a function of the fluence in Fig. 3b. A degradation can be observed as the fluence increases, with a degradation rate in good agreement with the results reported in the literature [reference]. Moreover, the J_{sc} degradation is found to be consistent with the EQE measurements (not shown here). Open-circuit voltage (V_{oc}) falls from 0.885 to 0.845 V accounting for 4.5 % degradation. This degradation correlates with an increase of one order of magnitude of the dark current density and is consistent with already published results [14], [16].
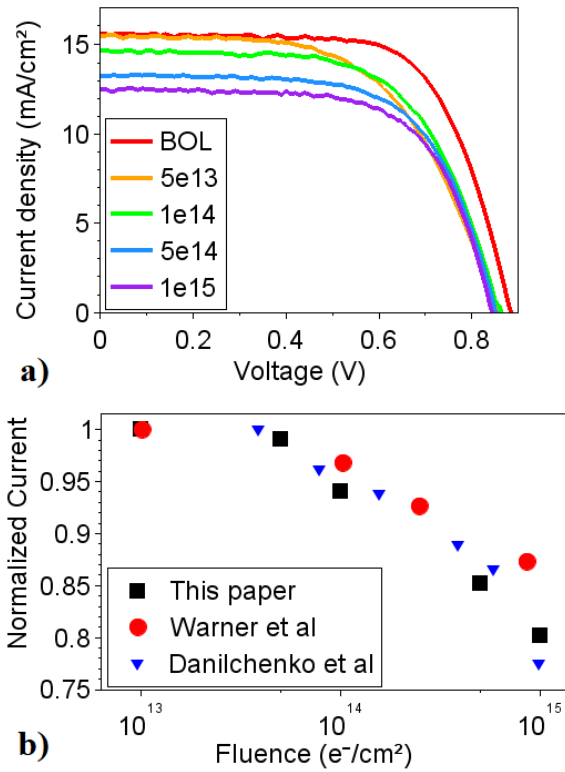
Fig. 3 a) *J-V* characteristics of GaAs G1 cell under AM0 light at 25°C and for different fluences b) Degradation of the photocurrent for G1 as a function of fluence, compared to literature data [14], [15]

The *J-V* curves of the InGaAsN cells were measured under spectrally-filtered light in order to reproduce the absorption of upper subcells in a MJSC. For that purpose, a Newport high-pass filter ($\lambda > 870$ nm) was placed within the optical path. Fig. 4a presents the evolution of the *J-V* curves of the A1 cell for different irradiation levels. The B1 and D1 cells exhibited the same *J-V* variation vs fluence as the A1 cell. Electron irradiation was found to be less detrimental to the InGaAsN cells than to the GaAs reference cell (G1), since the mean degradation of J_{sc} and V_{oc} after 10^{15} e⁻/cm² were lower than 6 % and 2 %, respectively. The degradations of J_{sc} for all dilute nitride cells are plotted in Fig. 4b. A clear difference in degradation rate can be observed between the cells irradiated directly at 1.10^{15} e⁻/cm² and the cells subjected to successive irradiations. That could be due to defect annealing (as discussed below) enhanced by uninterrupted irradiation. Otherwise, epitaxial growth conditions were not found to affect the degradation behavior of the cells, as J_{sc} and V_{oc} degradations for A, B, C and D were found to be roughly the same.
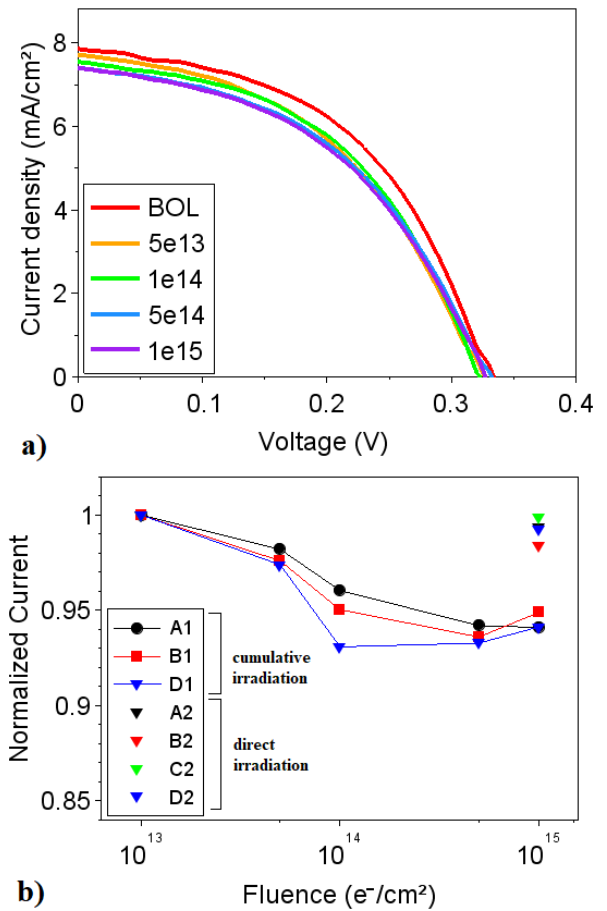

Fig. 4 a) *J-V* characteristics of InGaAsN A1 cell under AM0 > 870 nm light at 25°C and for different fluences b) Degradation of the photocurrent in InGaAsN cells as a function of fluence

We performed EQE measurements on solar cells directly irradiated at 10^{15} e⁻/cm². As it can be seen on the Fig. 5, irradiation has virtually no effects on the spectral response of InGaAsN cells and it can even be observed that the EQE signal in the range 650-1050 nm slightly increases after irradiation for cells A and B. However, this improvement disappears for longer wavelength which explains why it does not lead to higher J_{sc} under filtered AM0 light.

To describe the radiation hardness exhibited by InGaAsN cells, we propose three hypotheses. First, defect annealing and defect introduction occur simultaneously under irradiation. Indeed, annealing of growth defects during irradiation have already been reported for GaAs [17] and InGaAsN [18]. This phenomenon is based on the recombination-enhanced annealing mechanism coupled with the creation of vacancies in the lattice. Irradiation induces multiple ionizations in the material which in turn lead to a high carrier recombination rate. Carrier recombination can then locally bring enough energy to the lattice to anneal defects. However, for the defect recombination to be possible, vacancies need to be present in the lattice as it greatly enhances atomic diffusion [19]. Furthermore, the atomic diffusion of defects increases with temperature, which could explain why direct irradiation leads to lower degradation, as the sample might heat up more than it does under cumulative irradiation.
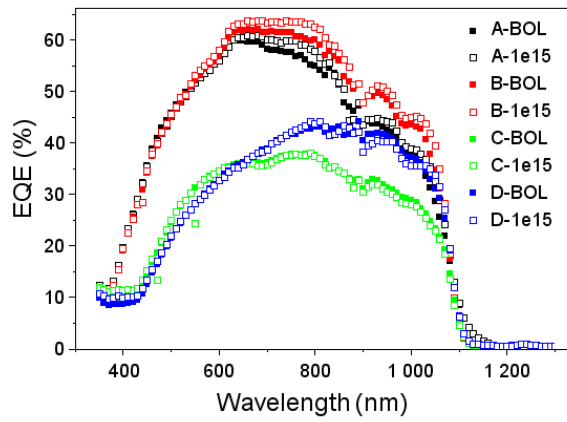
Fig. 5 EQE before and after 1 MeV electron irradiation for 4 InGaAsN cells

The second hypothesis to explain the radiation hardness of the cells is the predominance of growth defects over the irradiation-induced ones. Indeed, if at BOL the defect concentration is already high, then the contribution of the defects created during irradiation on the minority carrier diffusion length remain marginal – provided a low defect introduction rate – and would have a negligible impact on the cell's properties. This hypothesis is supported by the fact that a high density of N-related defects may be present in some dilute nitride materials, arising from the small size and the high electronegativity of the nitrogen anion [10], [20], [21]. This latter hypothesis underlies that the optical quality would be strongly affected, which does not seem to be the case with regard to the strong PL and EQE signals observed with our samples.

A third way to explain this radiation tolerance comes from the *pin* structure and the collection regime of the cells. As we said previously, the InGaAsN *pin* cells rely on the built-in electric field extending across the whole intrinsic layer to collect carriers, as a workaround for dilute nitride's low minority carrier diffusion length. Consequently, the decrease of this diffusion length through the introduction of defects has a smaller impact on the InGaAsN cells performance than it has on GaAs ones. A low J_{sc} degradation for GaAs *pin* solar cells has already been reported and attributed to this drift regime [22].

B. DLTS and PL evolution with irradiation

To assess the defect annealing explanation, i-DLTS measurements were performed on InGaAsN samples before and after 1 MeV electron irradiation. A Phystech DL8000 spectrometer and its analysis software were used for that matter. The reverse voltage was set to -1 V and we used a 0.5 ms filling pulse of 0 V. We measured the current transient between 10 and 50 ms after the end of the pulse. The DLTS spectra of as-grown and annealed samples from E and F wafers are shown in Fig. 6a. Although the crystal quality is different from one BOL sample to another - as depicted by the DLTS spectra - there is no significant difference between BOL and corresponding irradiated samples. Fig. 6b shows the deconvolution of two emission peaks that reveal the presence of two electron traps, with activation energy approximately

equal to 0.6 and 0.85 eV (as determined with the Arrhenius plot in Fig. 6c). As the bandgap energy of the DLTS sample is equal to 1.05 eV, the 0.6 eV trap appears to be quite deep and probably acts as an effective non-radiative recombination center. This defect is conjectured to be a nitrogen split interstitial $(N-N)_{As}$ since it is a typical defect in dilute nitrides and as its activation energy was theoretically calculated to be 0.66 eV below the conduction band [23]. Interestingly, as the amplitude of the DLTS signal is proportional to the defect concentration, it can be deduced that irradiation does not lead to a change of any of these defects concentration.
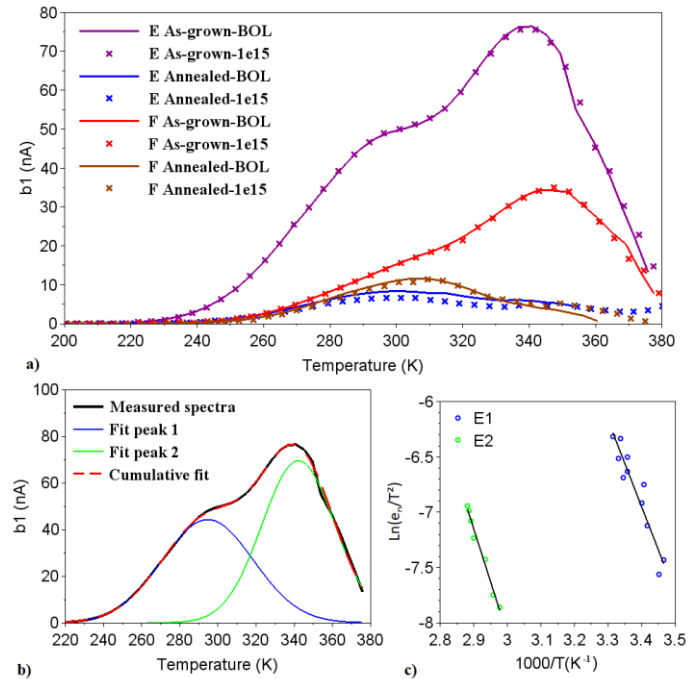

Fig. 6 a) DLTS spectra of samples before and after 1 MeV electron irradiation b) Deconvolution of the DLTS spectra of sample E As-grown-BOL in 2 emission peaks c) Arrhenius plot of E1 and E2 traps.

This result implies that the radiation hardness exhibited by the InGaAsN cells cannot be explained by the annealing of deep level growth defects such as $(N-N)_{As}$. However, it also shows that there is no sensible introduction of deep-level defects through the irradiation process, which supports our second hypothesis.

PL measurements were then made to assess the impact of irradiation on optical properties, as depicted in Fig. 7. The PL spectra were obtained at 300K with a 455 nm laser acting as the excitation source with a 15 mW/cm² power density. From Fig. 7 it can be seen that the PL signal increases after irradiation for as-grown samples whereas it remains constant or degrades for annealed ones. The fact that the PL increases after irradiation for as-grown samples means that there is less non-radiative recombination after irradiation. It points out the presence of growth-related shallow defects (not detectable with DLTS) and their curing during the irradiation process. This result correlates well with the slight increase of the EQE of unannealed cells after irradiation (Fig. 5). Additionally, we can see that the PL intensity of unannealed samples after irradiation gets closer to the intensity of annealed samples at

BOL. This suggests that the irradiation acts as the 750 °C RTP for curing shallow defects without however leading to the characteristic bandgap blueshift associated with thermal annealing of dilute nitrides.
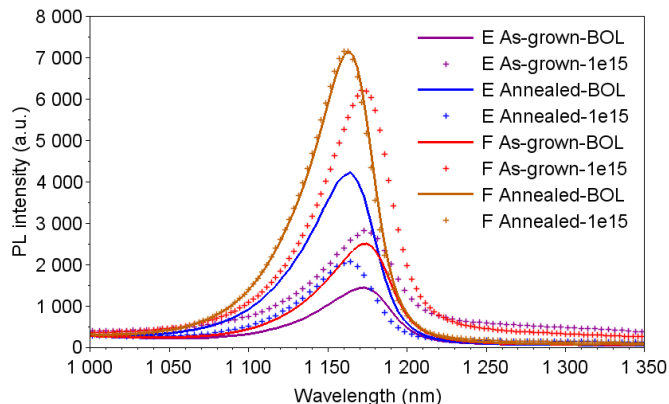

Fig. 7 PL spectra of samples before and after 1 MeV electron irradiation

The plateau-like degradation of the InGaAsN cells between 10^{14} and 10^{15} e⁻/cm² as well as the small J_{sc} recovery of B1 and D1 cells could then results from the annealing of these shallow defects. Moreover, the fact that the PL signal of the annealed samples does not increase (and even decreases in the case of wafer F) after irradiation can be explained by the change of InGaAsN preferential atomic bonding after RTP. Indeed, nitrogen atoms are reported to go from a Ga-N bonding configuration to a In-N one after annealing [24],[25], which could affect the defect energy formation and consequently the radiation hardness of the material.

IV. Conclusion

InGaAsN *pin* subcells and bulk layers were fabricated, electron-irradiated and characterized, showing a better resistance to 1 MeV electrons than GaAs cells. We have suggested three physical interpretations to explain this degree of tolerance based on both the specific material properties and the junction structure. DLTS and PL analysis on InGaAsN bulklayers show that the radiation hardness cannot be explained by the introduction and the annealing of deep-level defects. Indeed, the growth-defect density may be too important compared to the density of irradiation-induced defects. The PL enhancement and the slight EQE increase are then attributed to the annealing of shallow defects during irradiation.

Acknowledgment

References

[1] A.W. Bett, S.P. Philipps, S. Essig et al. "Overview about technology perspectives for high efficiency solar cells for space and terrestrial applications" *28th European Photovoltaic Solar Energy Conference and Exhibition*, 2013

[2] S.R. Kurtz, D. Myers, J.M. Olson "Projected performance of three- and four-junction devices using GaAs and GaInP," *Proceedings of the 26th IEEE PVSC*, p. 875, 1997

[3] M. Kondow, K. Uomi, A. Niwa et al. "GaInNAs: A Novel Material for Long-Wavelength-Range Laser Diodes with Excellent High-Temperature Performance" *Jpn. J. Appl. Phys.* vol. 35, pp.1273-1275, 1996

[4] D.J. Friedman, J.F. Geisz, S.R. Kurtz, J.M. Olson "1-eV solar cells with GaInNAs active layer" *J. Cryst. Growth* vol. 195, pp.409-415, 1998

[5] J.F. Geisz, D.J. Friedman "III–N–V semiconductors for solar photovoltaic applications," *Semiconductor Science and Technology* vol. 17, pp. 769-777, 2002

[6] M. Wiemer, V. Sabnis, H. Yuen "43.5% efficient lattice matched solar cells", *Proceedings of SPIE*, vol. 8108, 2011

[7] S. Kurtz, R.R. King, K.M. Edmondson, D.J. Friedman, N.H. Karam "1-MeV-electron irradiation of GaInAsN cells" *Conf. Record of the 29th IEEE PVSC*, pp. 1006-1009, 2002

[8] A. Khan, J. Gou, M. Imazumi, M. Yamaguchi "Interaction of electron irradiation with nitrogen-related deep levels in InGaAsN" *Appl. Phys. Lett.*, 043503, vol. 91, 2007

[9] A. Khan, J. Gou, R.C. Lam et al "DLTS analysis of radiation-induced defects in InGaAsN solar cell structures" *IEEE 4th WCPEC*, pp. 1858-1860, 2006

[10] V. Polojarvi, A. Aho, A. Tukiainen et al. "Influence of As/group-III flux ratio on defects formation and photovoltaic performance of GaInNAs solar cells," *Sol. Energy Mater. Sol. Cells* vol. 149, pp. 213–220, 2016

[11] M.M. Wilkins, J. Gupta, A. Jaouad et al. "Design of thin InGaAsN(Sb) n-i-p junctions for use in four-junction concentrating photovoltaic devices" *J. Photonics Energy* vol. 7(2), 2017

[12] A. Tukiainen, A. Aho, G. Gori et al. "High-efficiency GaInP/GaAs/GaInNAs solar cells grown by combined MBE-MOCVD technique" *Prog. Photovolt: Res. Appl.* vol.24, pp. 914–919, 2016

[13] S. Duzellier, L. Artola, G. Hubert et al. "AXEL lab.: representative ground simulation for investigating radiation effects in materials and electronics" *17th European Conference on Radiation and Its Effects on Components and Systems (RADECS)*, 2007

[14] J.H. Warner, S.R. Messenger, R.J. Walters et al. "Correlation of Electron Radiation Induced-Damage in GaAs Solar Cells" *IEEE Transactions on Nuclear Science* vol. 53, pp. 1988-1994, 2006

[15] B. Danilchenko, A. Budnyk, L. Shpinar et al. "1MeV electron irradiation influence on GaAs solar cell performance" *Sol. Energy Mater. Sol. Cells* vol. 92, pp. 1336–1340, 2008

[16] *GaAs Solar Cell Radiation Handbook*, Jet Propulsion Laboratory, Pasadena, California, USA, 1996, Chapter 6

[17] D Pons, C Bourgoin "Irradiation-induced defects in GaAs" J. *Phys. C: Solid State Phys*. vol. 18, pp. 3839-3871, 1985

[18] E.M. Pavelescu, R. Kudrawiec, J. Puustinen, A.Tukiainen, M.Guina "Effects of 7-MeV electron irradiation on photoluminescence from 1-eV GaInNAs-on-GaAs epilayers" *Journal of Luminescence* vol. 136 (2013) 347–350

[19] J.C. Bourgoin, J.W. Corbett "Enhanced diffusion mechanisms" *Radiation Effects* vol. 36, pp. 157-188, 1978

[20] R. Kaplar, D. Kwon, S.A. Ringel et al. "Deep levels in p- and n-type InGaAsN for high-efficiency multi-junction III-V solar cells," *Sol. Energy Mater. Sol. Cells* vol. 69, pp. 85–91, 2001

[21] A. Khan, S.R. Kurtz, S. Prasad, S.W. Johnston, J. Gou "Correlation of nitrogen related traps in InGaAsN with solar cell properties," *Appl. Phys. Lett.* vol. 90, 2007

[22] T. Ohshima, S. Sato, M. Imaizumi et al. "Change in the electrical performance of GaAs solar cells with InGaAs quantum dot layers by electron irradiation" *Sol. Energy Mater. Sol. Cells* vol. 108, pp. 263–268, 2013

[23] S. B. Zhang and S. H. Wei, "Nitrogen solubility and induced defect complexes in epitaxial GaAs:N" *Phys. Rev. Lett.*, vol. 86, no. 9, pp. 1789–1792, 2001

[24] K. Volz, D. Lackner, I. Németh et al. "Optimization of annealing conditions of (GaIn)(NAs) for solar cell applications" *Journal of Crystal Growth* vol.310, pp. 2222-2228, 2008

[25] K. Uno, M. Yamada, I. Tanaka, O. Ohtsuki, T. Takizawa "Thermal annealing effects and local atomic configurations in GaInNAs thin films" *Journal of Crystal Growth* vol.278, pp. 214-218, 2005